

## Direct Scattering, Trapping, and Desorption in Atom-Surface Collisions

Guoqing Fan<sup>1</sup> and J. R. Manson<sup>1,2</sup>

<sup>1</sup>*Department of Physics and Astronomy, Clemson University, Clemson, South Carolina, 29634, USA*

<sup>2</sup>*Donostia International Physics Center (DIPC), P. Manuel de Lardizabal 4, 20018 San Sebastian, Spain*

(Received 3 April 2008; published 8 August 2008)

Maxwell is credited as the first to invoke the assumption that an impinging gas beam scatters from a surface with a direct contribution exhibiting little change in state and a trapping-desorption fraction that desorbs in equilibrium [J. C. Maxwell, Phil. Trans. R. Soc. London **170**, 231 (1879)]. Here a classical mechanical scattering theory is developed to describe direct scattering, trapping, and subsequent desorption of the incident beam. This theory allows a rigorous test of the Maxwell assumption and determines the conditions under which it is valid. The theory also gives quantitative explanations of important new experimental measurements [K. D. Gibson, N. Isa, and S. J. Sibener, J. Chem. Phys. **119**, 13083 (2003)] for direct and trapping-desorption scattering of Ar atoms by a self-assembled layer of 1-decanethiol on Au(111).

DOI: 10.1103/PhysRevLett.101.063202

PACS numbers: 34.35.+a, 34.50.-s, 82.20.Rp

Maxwell is credited with being the first to discuss in quantitative terms the process of trapping and desorption of atomic and molecular projectiles upon colliding with a surface. As a solution to his well-known problem that a gas of elastic scatterers will not by itself come to equilibrium, he proposed in a paper published in the last year of his life that, when the gas particles collided with the walls of the container, a fraction would be directly scattered with little change in state, while the remaining fraction would be trapped and then subsequently “evaporated” in equilibrium at the temperature of the container [1].

Trapping-desorption processes are highly probable events in the interaction of thermal energy atoms and molecules with surfaces, and the Maxwell assumption is often invoked in order to describe the desorbing fraction as a near-equilibrium distribution [2–4]. However, although it is often experimentally observed that the desorbed fraction obeys near-equilibrium properties, the conditions under which such an assumption is valid have not up to now been adequately verified with reliable theoretical calculations. In fact, classical trajectory simulations have indicated that trapping can lead to apparent chaotic behavior in which a small change in incident conditions can lead to large deviations in the final desorption trajectory [5].

The purpose of this work is twofold. First, we test the Maxwell assumption of equilibrium for the trapping-desorption fraction using realistic calculations for a straightforward model of the gas-surface potential and determine the conditions under which such an assumption is valid. Second, we demonstrate that the same potential model can explain modern high-precision energy-resolved scattering measurements.

The calculations are carried out using classical mechanics, which is justified for many systems of interest in rarefied gas-surface dynamics. A classical treatment means that the results will describe heavy mass atoms at higher energies, meaning typically hyperthermal speeds, and surfaces at high temperatures where quantum mechanical

effects are not dominant. The gas projectile is taken to be an atom, and its interaction potential is taken to be a strongly repulsive surface barrier with an attractive square well for the physisorption potential. The use of a square well to approximate the attractive, slowly varying van der Waals potential is also reasonable when used with a classical calculation, since it gives a good description of the two primary effects upon entering the well which are an increase in energy and a refraction of the atom toward steeper angles to the surface. Similar potentials have proved useful in quantitatively explaining experimental data under conditions in which direct scattering is dominant [6,7] and in theoretical discussions of trapping or desorption in the case of one-dimensional motion [8].

A surface scattering event can be described through a differential reflection coefficient, written as  $dR(\mathbf{p}_f, \mathbf{p}_i)/dE_f d\Omega_f$ , which gives the fraction of an incident beam of momentum  $\mathbf{p}_i$  that is scattered into the small energy interval and the small solid angle in the direction of the final scattered momentum  $\mathbf{p}_f$ . For the present calculations, the most appropriate differential reflection coefficient for a single collision is that for an atomic projectile colliding with a surface of discrete scattering centers of mass  $M$  whose initial momenta are distributed in an equilibrium distribution at temperature  $T_S$ . This is given by [9–11]

$$\frac{dR^0(\mathbf{p}_f, \mathbf{p}_i)}{dE_f d\Omega_f} = \frac{m^2 |\mathbf{p}_f|}{8\pi^3 \hbar^4 p_{iz} N_D^0} |\tau_{fi}|^2 \left( \frac{\pi}{k_B T_S \Delta E_0} \right)^{1/2} \times \exp \left\{ - \frac{(E_f - E_i + \Delta E_0)^2}{4k_B T_S \Delta E_0} \right\}, \quad (1)$$

where  $\Delta E_0 = (\mathbf{p}_f - \mathbf{p}_i)^2 / 2M$  is the recoil energy,  $p_{iz}$  is the  $z$  component of the incident momentum,  $k_B$  is the Boltzmann constant, and  $|\tau_{fi}|^2$  is the form factor which depends on the interaction potential. To lowest order, the amplitude  $\tau_{fi}$  is identified as the transition matrix element

of the elastic interaction potential extended off the energy shell [12], and for this work we use the value appropriate for hard sphere scattering which is a constant.

Once a beam of incoming atoms interacts with the surface, a fraction will be directly scattered, while the remainder will be trapped in the potential well. Of the trapped fraction, some will lose sufficient energy to be actually trapped in the well with negative total energy, while others, even though they have positive total energy, will scatter at angles sufficiently close to grazing, so that they will have negative energy associated with motion normal to the surface and will be deflected back towards the surface by the attractive part of the well. This latter, positive energy part of the trapped particles is often called the chattering fraction. The trapped portion of the incident beam particles will continue to have interactions with the surface, and with each subsequent collision some will receive enough energy and will be projected sufficiently close to the surface normal that they can escape, while the remainder will continue to be trapped. Eventually, in a closed system, all particles initially trapped will ultimately desorb from the surface, although for low temperatures and deep potential wells this may take a very large time.

For the model considered here, an iterative algorithm is carried out in momentum space, and the problem is discretized by separating all scattered particles into energy and angular bins. All of the trapped particles are followed as they continue to have collisions with the surface, and at each iteration the negative energy fraction, the chattering fraction, and that fraction which is desorbed are recalculated. In this manner, the energy distribution of the slowly diminishing trapped particle fraction as well as the energy and angular distribution of the desorbed (or scattered) particles are followed, and an average trapping time is calculated. By following the initial direct scattering and the sum of all of the subsequently desorbed particles, the approach to equilibrium of the trapping-desorption fraction can be monitored.

Based on the zeroth order differential reflection coefficient  $dR^0(\mathbf{p}_f, \mathbf{p}_i)/dE_f d\Omega_f$  of Eq. (1) to describe single scattering, and taking multiple scattering events to be successive convolutions of single scattering collisions, the total differential reflection coefficient after  $n$  such collision iterations is written schematically as

$$\begin{aligned} \frac{dR^n(\mathbf{p}_f, \mathbf{p}_i)}{dE_f d\Omega_f} &= \frac{dR^0(\mathbf{p}_f, \mathbf{p}_i)}{dE_f d\Omega_f} \\ &+ \int dE_b d\Omega_b \frac{dR^0(\mathbf{p}_f, \mathbf{p}_b)}{dE_f d\Omega_f} \frac{dR^0(\mathbf{p}_b, \mathbf{p}_i)}{dE_b d\Omega_b} \\ &+ \int dE_b d\Omega_b \frac{dR^0(\mathbf{p}_f, \mathbf{p}_b)}{dE_f d\Omega_f} \frac{dR^1(\mathbf{p}_b, \mathbf{p}_i)}{dE_b d\Omega_b} + \dots \\ &+ \int dE_b d\Omega_b \frac{dR^0(\mathbf{p}_f, \mathbf{p}_b)}{dE_f d\Omega_f} \frac{dR^{n-1}(\mathbf{p}_b, \mathbf{p}_i)}{dE_b d\Omega_b}, \quad (2) \end{aligned}$$

where the intermediate integrations in the higher order terms are carried out only over those energies and angles that pertain to particles trapped in the bound states.

Figure 1 shows an example calculation of the evolution of the energy distribution as a function of the number  $n$  of iterations for the case of argon scattering from a tungsten surface. The incident angle is  $45^\circ$ , the incident energy is 1 meV, the well depth is chosen to be 80 meV, and the surface temperature is 303 K. The dotted curve shows the continuum energy distribution after the first iteration, which is the second collision with the surface. The trapping fraction is  $P^1 = 0.954$ , indicating that 95.4% of the incident particles remain trapped in the potential well. The dashed-dotted and two different dashed curves show the evolution of the continuum scattered distribution after increasing numbers of iterations of 5, 50, and 500. After 500 iterations, there is still approximately one-third of the incident particles trapped. After 2124 iterations, the trapped fraction drops below the arbitrary threshold of 1% of the incident particles, and the energy distribution at all final scattered angles becomes very nearly the expected equilibrium Knudsen flux.

The evolution of a system towards a final equilibrium distribution as a function of potential well depth  $D$  is shown in Fig. 2. The parameters are similar to the Ar/W system of Fig. 1 above, the projectile is incident normally at  $\theta_i = 0^\circ$  with  $E_i = 1$  meV and  $T_s = 303$  K, but completely converged calculations (meaning less than 1% of the incident particles remain trapped) are shown for the three different well depths of 20, 50, and 80 meV. This figure shows clearly that, even if the incident energy is very small and the initially trapped fraction is large, the total scattered distribution does not approach equilibrium unless

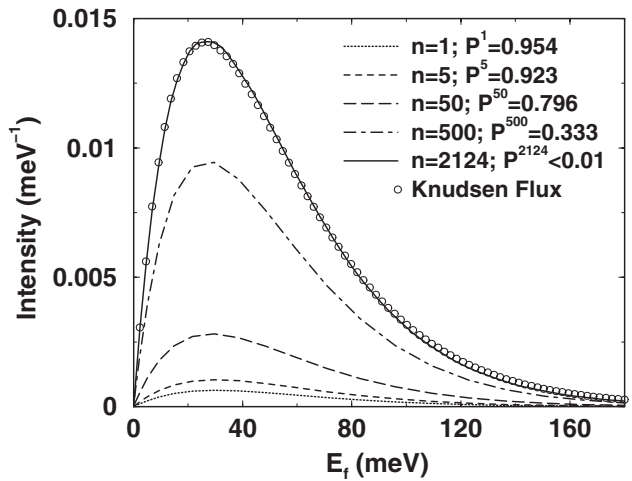


FIG. 1. Argon scattering from a tungsten surface at low incident energy: the evolution of the final energy distribution for particles scattered into the continuum states after a specified number of iterations. Five curves of the final distributions for the iteration numbers  $N = 1, 5, 50, 500$ , and 2124 are shown. For comparison, a Knudsen equilibrium flux is given as open circles.

the adsorption well is sufficiently deep to cause long average trapping times. For the shallow well of 20 meV with an initial trapping fraction of 0.83 and average desorption time of about  $5.3 \times 10^{-10}$  s (based on a well width of 3 Å), the final distribution deviates strongly from an equilibrium distribution. It is only when the well depth is increased to about 80 meV, with the corresponding average trapping time of about  $4.4 \times 10^{-9}$  s, that equilibrium conditions are achieved.

The response of the angular distribution is given in Fig. 3. The progression towards an equilibrium  $\cos\theta_f$  distribution is clearly evident with increasing well depth, although the expected behavior is achieved more slowly than that of the energy distribution exhibited in Fig. 2. For the rather large value of  $D = 200$  meV, for which the average trapping time is  $6.4 \times 10^{-7}$  s, at  $\theta_f = 0^\circ$  the calculated value is 96% of the cosine maximum.

The examples shown in Figs. 1–3, as well as many other calculations that we have carried out [13], demonstrate that this potential model can clearly indicate the conditions for which the Maxwell assumptions are valid. However, the mere fact that these calculations can indicate the conditions under which the trapping-desorption fraction appears as a nearly equilibrium distribution is not sufficient to demonstrate that such conditions are realistic. In order to be convincing, calculations with the same potential model should be capable of explaining real experimental measurements. To demonstrate this ability, we compare our calculations with recent high-precision energy-resolved data for the scattering of Ar atoms from a well-ordered self-assembled monolayer of the polymer 1-decanethiol adsorbed on Au(111) [2]. This experiment showed that, for well-defined beams of Ar incident over a large range of energies and angles, the scattered distributions could be described by a combination of two features: a direct scat-

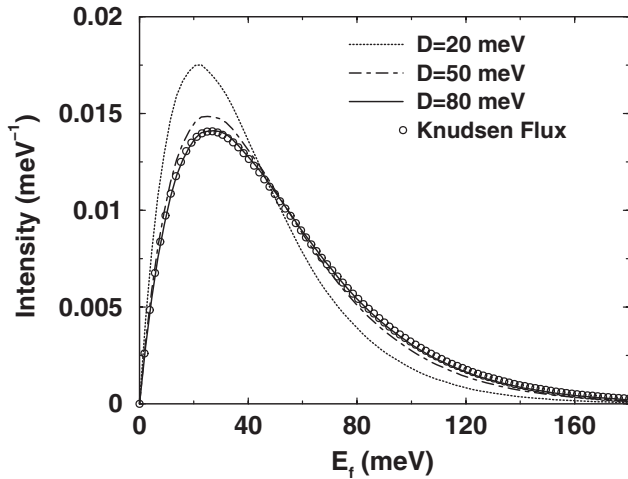


FIG. 2. Final energy distributions for an Ar/W system with well depths  $D = 20, 50$ , and  $80$  meV. A Knudsen distribution is shown as open circles.

tering fraction and a trapping-desorption fraction that was modeled as being approximately in equilibrium with the surface.

Three examples of data measured at an incident energy of 365 meV and a temperature of 135 K are shown in Fig. 4 for different combinations of incident and final angles. The upper panel for  $\theta_i = 45^\circ$  and  $\theta_f = 50^\circ$  and the lower panel showing  $\theta_i = 30^\circ$  and  $\theta_f = 80^\circ$  present a clear distinction between the rather sharp peak at a short time of flight (TOF) and a broader shoulder at larger times. The appearance of a distinct direct scattering peak is largely due to the fact that the incident energy is larger than the depth of the potential well. The solid curves in Fig. 4 are calculations carried out with an effective mass ratio  $\mu = 0.56$  obtained by fitting to the high-energy direct scattering peak and a well depth  $D = 35$  meV obtained by fitting to the low-energy tail. The calculations explain the data quite well, and the dashed-dotted curves show clearly the separation between the direct and trapping-desorption fractions. The value  $D = 35$  meV is in agreement with that of the potential energy function for this system developed in Ref. [2] in which the physisorption well depth varied from 33 to 67 meV depending on the relative position within the surface unit cell over the self-assembled layer. The effective mass ratio corresponds to a surface mass of 71 amu, somewhat smaller than the 174.3 amu mass of the 1-decanethiol molecule, and is slightly smaller than the value  $\mu = 0.62$  obtained in Ref. [2] by a fitting based on the Baule equations for hard sphere scattering. The results are quite sensitive to the effective mass, and calculations with  $\mu = 0.62$  produce a direct scattering peak positioned at a TOF time about 10  $\mu$ s shorter or 15 meV higher in energy.

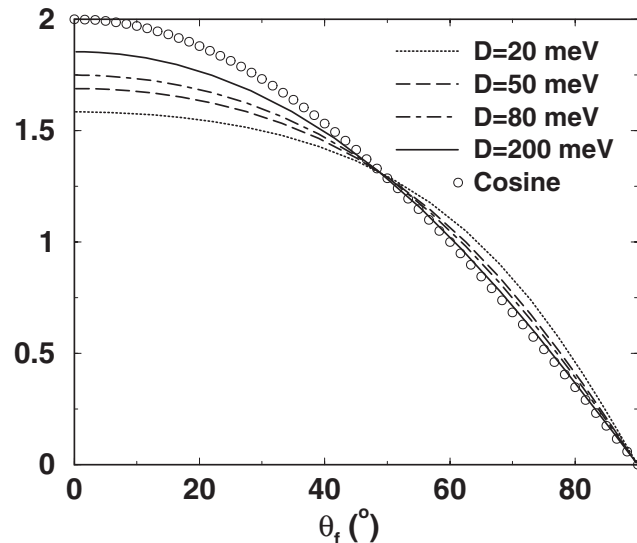


FIG. 3. The polar angular distribution for the same system shown in Fig. 2. The evolution towards the Knudsen distribution, displayed as open circles, is shown for a series of increasing well depths.

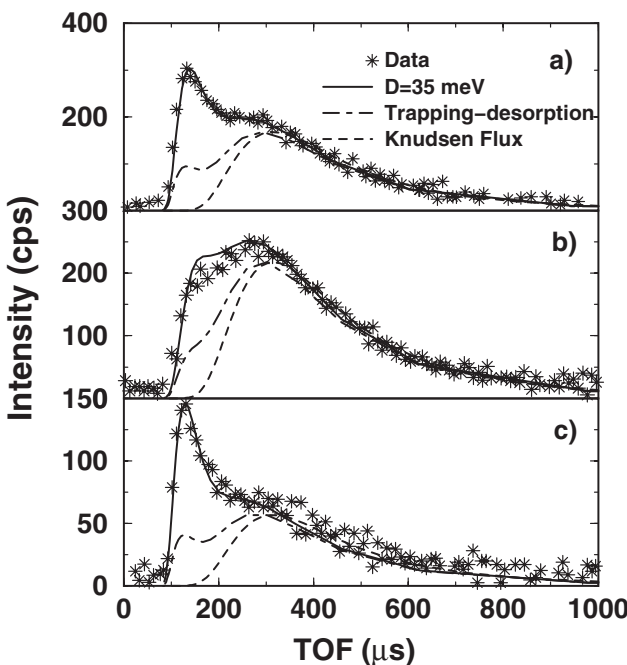


FIG. 4. Intensity versus TOF for Ar scattering from a 1-decanethiol layer on Au(111) with  $E_i = 365$  meV: (a)  $\theta_i = 45^\circ$  and  $\theta_f = 50^\circ$ , (b)  $\theta_i = 30^\circ$  and  $\theta_f = 50^\circ$ , and (c)  $\theta_i = 30^\circ$  and  $\theta_f = 80^\circ$ . The solid curves are calculations with  $\mu = 0.56$  and  $D = 35$  meV, the dashed-dotted curves are the trapping-desorption fractions, and the short-dashed curves are the Knudsen distribution.

Also shown in Fig. 4 are the trapping-desorption fraction and the Knudsen curves. Interestingly, the trapping-desorption fraction itself has a multiple-peaked structure with a small subpeak appearing at almost the same final energy as the direct scattering contribution. This small high-energy subpeak comes from the first few collisions as the initially adsorbed particles travel in the potential well. These first few collisions have a high probability of ejecting particles back into the continuum with relatively little loss of energy compared to the direct scattering fraction. However, it is clear that the largest part of the trapping-desorption fraction emerges at thermal energies, and the long, low-energy tail closely resembles that of the Knudsen distribution.

Our extended calculations [13] provide an excellent description of all of the scattered spectra presented in Ref. [2], and the relative intensity of the direct to trapping-desorption contributions allows for an estimate of the average physisorption well depth of the interaction potential. Our calculations also confirm two other important observations of Ref. [2]. The first of these is that, at the lowest energy measured, which was 65.3 meV, the scat-

tered TOF spectra exhibited only a single broad peak at thermal energies, and the second was that, even at the highest measured incident energies of 582 meV, if the incident angle was near-normal, there was no clear separation of the scattered TOF spectra into direct and trapping-desorption peaks. An example of this latter effect is the lack of clear separation of the two features in the middle panel of Fig. 4 for which the incident angle is  $30^\circ$ . Our calculations confirm these observations, both at low energies and at high energies if the incident angle is near-normal, the initial trapping fraction is large, so large in fact that the direct scattering contribution becomes small.

Since this theory is demonstrably useful for explaining currently available high-precision experimental data, it should clearly be useful in predicting the validity of the well-accepted Maxwell assumption for the trapping-desorption fraction in gas-surface collisions. Our calculations indicate that Maxwell's assumption is strictly valid only when the overwhelming majority of incident particles are trapped, the average trapping times are long, and the direct scattering is correspondingly small. When the direct and trapping-desorption contributions are comparable in total intensity, the trapping-desorption part can deviate considerably from an equilibrium Knudsen distribution, but, since it is emitted in the thermal energy range, the Maxwell assumption remains a useful tool for its approximate description.

This work was supported in part by the U.S. Department of Energy under Grant No. DE-FG02-98ER45704.

- [1] J. C. Maxwell, Phil. Trans. R. Soc. London **170**, 231 (1879).
- [2] K. D. Gibson, N. Isa, and S. J. Sibener, J. Chem. Phys. **119**, 13 083 (2003).
- [3] B. Scott Day, Shelby F. Shuler, Adonis Ducre, and John R. Morris, J. Chem. Phys. **119**, 8084 (2003).
- [4] M. K. Ferguson, J. R. Lohr, B. S. Day, and J. R. Morris, Phys. Rev. Lett. **92**, 073201 (2004).
- [5] R. Guantes, S. Miret-Artés, and F. Borondo, Phys. Rev. B **63**, 235401 (2001).
- [6] A. Muis and J. R. Manson, J. Chem. Phys. **107**, 1655 (1997).
- [7] W. H. Hayes and J. R. Manson, J. Chem. Phys. **127**, 164714 (2007).
- [8] Guoqing Fan and J. R. Manson, Phys. Rev. B **72**, 085413 (2005).
- [9] A. Sjölander, Ark. Fys. **14**, 315 (1959).
- [10] D. A. Micha, J. Chem. Phys. **74**, 2054 (1981).
- [11] J. R. Manson, Phys. Rev. B **43**, 6924 (1991).
- [12] J. R. Manson, V. Celli, and D. Himes, Phys. Rev. B **49**, 2782 (1994).
- [13] Guoqing Fan and J. R. Manson (to be published).